REPORT DOCUMENTATION PAGE

Form Approved
OMB No. 0704-0188

1. AGENCY USE ONLY (*Leave blank*)

2. REPORT DATE

3. REPORT TYPE AND DATES COVERED
FINAL/30 SEP 93 TO 29 SEP 94

4. TITLE AND SUBTITLE
DEPSCOR92 - WIDE FIELD SPECTRAL IMAGER

5. FUNDING NUMBERS
3484/BS
F49620-93-1-0559

6. AUTHOR(S)
PROFESSOR JOHN A KIELKOPF

7. PERFORMING ORGANIZATION NAME(S) AND ADDRESS(ES)
DEPARTMENT OF PHYSICS
UNIVERSITY OF LOUISVILLE
LOUISVILLE, KENTUCKY 40292

8. PERFORMING ORGANIZATION REPORT NUMBER
AFOSR-TR- 95 - 0220

9. SPONSORING/MONITORING AGENCY NAME(S) AND ADDRESS(ES)
AFOSR/NM
110 DUNCAN AVE, SUTE B115
BOLLING AFB DC 20332-0001

10. SPONSORING/MONITORING AGENCY REPORT NUMBER
F49620-93-1-0559

11. SUPPLEMENTARY NOTES

12a. DISTRIBUTION/AVAILABILITY STATEMENT

APPROVED FOR PUBLIC RELEASE: DISTRIBUTION IS UNLIMITED

12b. DISTRIBUTION CODE

13. ABSTRACT (*Maximum 200 words*)

The wide Field Spectral Imager (WISPI) project was designed to provide a new capability for measuring the spectrum of the sky across fields of view much larger than the full moon. The instrument which we proposed would use a high speed optical system to form an image on the entrance slit of a matching stigmatic spectrometer, which would then disperse a spectrum of a strip of the sky onto a sensitive two-dimensional detector. A separate imaging system would be used for pointing and tracking, and both instruments would be on a computer controlled mounting that would permit automated data acquisition. Data from the instrument could be acquired remotely and then stored and analyzed on a high speed workstation.

19950331 123

14. SUBJECT TERMS

15. NUMBER OF PAGES

16. PRICE CODE

17. SECURITY CLASSIFICATION OF REPORT	18. SECURITY CLASSIFICATION OF THIS PAGE	19. SECURITY CLASSIFICATION OF ABSTRACT	20. LIMITATION OF ABSTRACT
UNCLASSIFIED	UNCLASSIFIED	UNCLASSIFIED	SAR(SAME AS REPORT)

Wide Field Spectral Imager

Final Technical Report
DEPSCOR92 USAF F49620-93-1-0559

John Kielkopf
Department of Physics
University of Louisville
Louisville, KY 40292

February 25, 1995

1 Introduction

The Wide Field Spectral Imager (*WISPI*) project was designed to provide a new capability for measuring the spectrum of the sky across fields of view much larger than the full moon. The instrument which we proposed would use a high speed optical system to form an image on the entrance slit of a matching stigmatic spectrometer, which would then disperse a spectrum of a strip of the sky onto a sensitive two-dimensional detector. A separate imaging system would be used for pointing and tracking, and both instruments would be on a computer controlled mounting that would permit automated data acquisition. Data from the instrument could be acquired remotely and then stored and analyzed on a high speed workstation.

Construction of this system began in October 1993, and continued with these highlights:

October 1993 Ordering of detectors, computers, and other long lead-time components.

November 1993 Completion of final optical design; ordering of optical components.

December 1993 Completion of final mechanical design; ordering of mechanical components; start of fabrication.

January 1994 Installation of data processing computer system; start of software development.

February 1994 Delivery of primary detector system and control computer.

March 1994 Delivery of drive motors and control software development package.

May 1994 Completion of instrument fabrication and metal finishing.

June 1994 Final assembly; mechanical testing; production of control software.

July 1994 Control software completed; instrument moved to remote site; light shields and baffles installed; first sky tests undertaken: observations of the impact of Comet Shoemaker-Levy with Jupiter recorded on July 18; wiring harnesses completed.

August 1994 Tracking control detector delivered; autotracking programs debugged; first nebular spectra recorded; systematic stellar spectral studies initiated: spectrometer for intermediate fields of view delivered.

October 1994 Order separation filter installed; spectrum of Vega recorded; preliminary absolute calibration of spectral and spatial response established.

November 1994 Instrument moved to an elevated platform to provide full sky view; airglow measurements made for sensitivity limit studies; weak emission from the Rosette nebula detected.

December 1994 Faint emission from hydrogen detected near the Pleiades; approximate stellar magnitude calibration established.

February 1995 Searches for extended faint emission initiated.

The instrument is now fully functional at our site. Provision has been made to package and transport it to alternative sites with darker skies, or to low latitude sites to measure the southern sky. Negotiations are also now underway to establish operating support for the Air Force needs as outlined in the proposal.

2 Instrument Construction

A photograph of the completed instrument is shown in Figs. 1 and 2. This instrument is augmented for higher spatial resolution by configuring it to couple to a larger telescope which is not shown. The characteristics of *WISPI* will be discussed in the following section. In the course of setting the final design, some modifications were made to the proposed design, but the performance goals were met or exceeded. The cost of the completed package was less than the grant budget. A analysis of the cost is sorted by category.

The items identified in this table are grouped by function, as in the proposal.

1. Imaging and collimating optics
2. Spectroscopic components
3. Detectors
4. Mounting and drive components
5. Instrument control computer
6. Image analysis computer
7. Miscellaneous

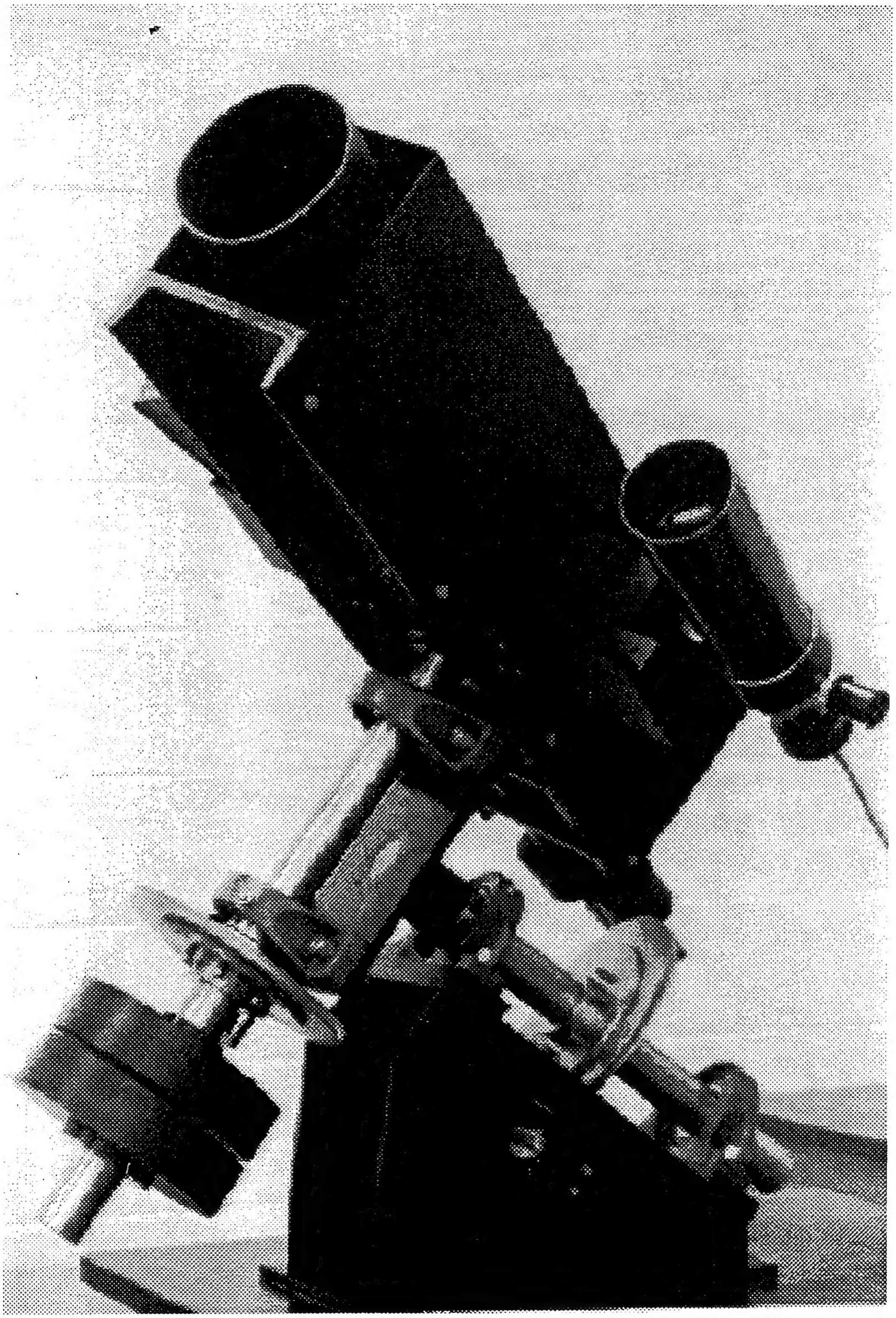

Figure 1: The completed wide field spectral imager (*WISPI*) prior to its move to the observatory.

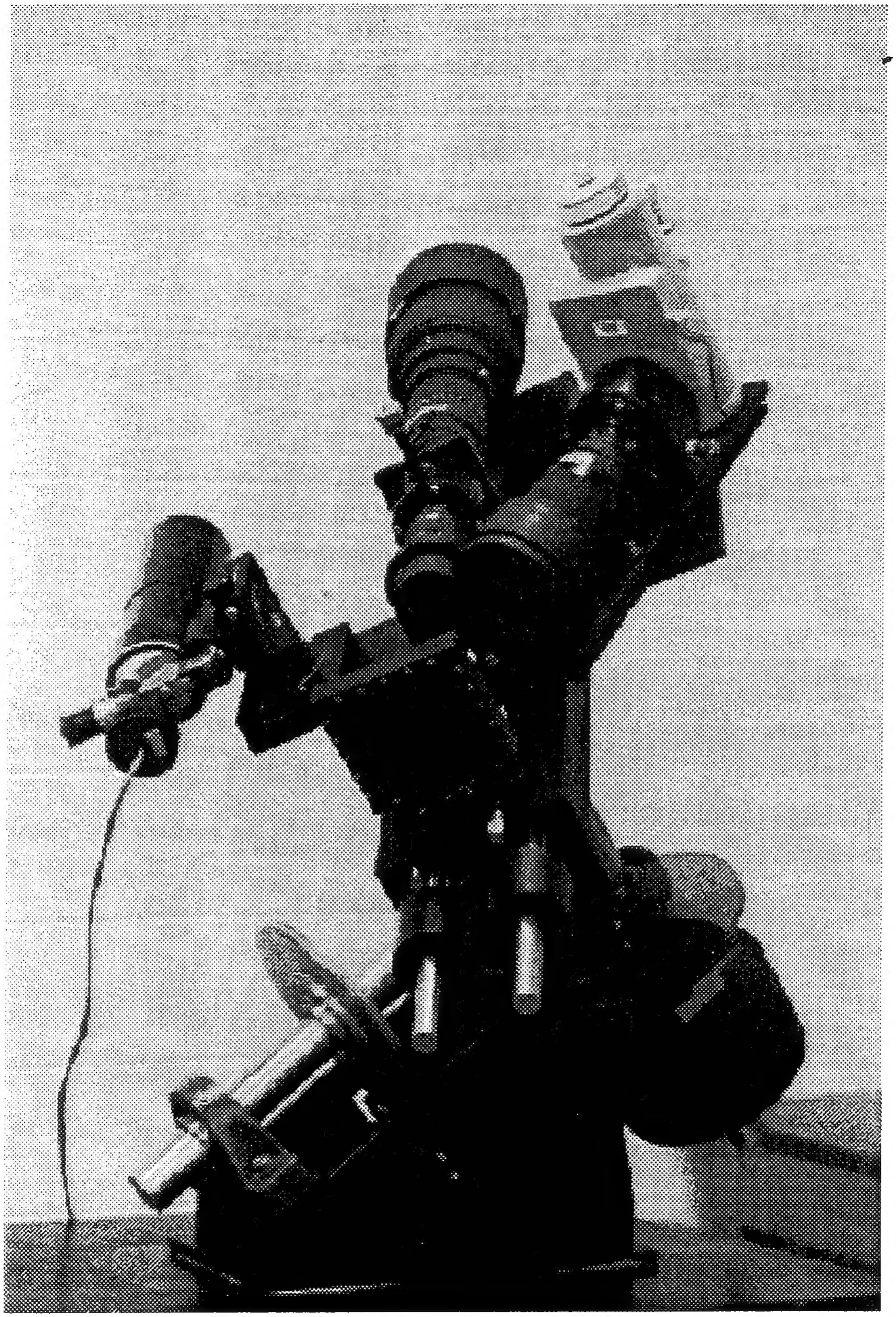

Figure 2: The wide field spectral imager (*WISPI*) with its covers removed to show the internal optical system. Light from the sky enters the large 400 mm lens at top center. is imaged on the slit, collimated by the smaller 180 mm lens, and diffracted by the grating at the bottom toward the 200 mm lens and CCD camera on the right. The Questar tracking telescope is on the left.

Item	Component	Supplier	Cost†
1.a	200 mm f/2.0 Nikor lens	K&R	$11,648
1.b	400 mm f/2.8 Nikor lens		
1.c	(2) 180 mm f/2.8 Nikor lenses		
1.d	3.5″ Questar telescope	Moore Observatory	0
2.a	0.25 m Spectrograph	Chromex	8,466
2.b	Diffraction Grating	Milton Roy	1,578
2.c	Spex precision bilateral slit	Moore Observatory	0
3.a	Tektronix 1024 × 1024 CCD	Princeton Instruments	48,195
3.b	Texas Instruments 323 × 242 CCD	SBIG	1,820
4.a	Mounting	Physics shop	0
4.b	Stepping motor drives	Aerotech	4,036
4.c	Precision rotating stages	Newport	3,058
4.d	(2) 10″ worm gears	Byers	1,825
5.a	32-bit PC	Digital	5680
5.b	Forth software	LMI	155
5.c	Hewlett Packard DAT tape drive	Cranel	1,514
5.d	Hewlett Packard laser printer	CBM	1,670
6.a	Workstation	Digital	21,732
6.b	System software	Digital	0
6.c	Hewlett Packard DAT tape drive	Cranel	1,514
6.d	Hewlett Packard inkjet printer	CBM	2,590
6.e	Disk drive	Tribeca	1,015
6.f	Disk drive	Tristar	1,585
7.a	NASA Digitized Sky Survey	Astr. Soc. Pacific	2,900
7.b	Storage cases	Specialized Products	1,481
7.c	Small parts		1,677
Total			$124,139

†Invoiced price including shipping charges rounded to the nearest $1.

In the following we consider each of these and discuss the differences between them and the corresponding entry in the proposal.

1.a The 200 mm f/2.0 Nikor lens is the the camera lens for imaging the dispersed spectrum or alternatively a wide field lens for direct imaging. In the preliminary design we were to use this lens for guidance and reference wide field image work only. In the revised design, this lens is used normally as a collimator for light dispersed from a plane grating in a spectrometer of our own design. This change gave us higher angular resolution than we were able to obtain in any commercial spectroscopic instrument, and a much faster optical system. The camera lens and CCD may be switched from pointing at the grating to pointing at the sky in the two different modes of operation.

1.b The 400 mm f/2.8 Nikor is a faster version of the lens originally specified. By using this lens, or alternatively one of the two lenses in **1.c**, we obtain an f/2.8 acceptance beam rather than the original f/4.0 . This is fully an improvement of 1 f-stop, a factor of 2 in energy/area-time at the CCD detector. By negotiation with the vendor we were able to acquire this improved lens and the others in **1.a - 1.c** for only $448 more than the budgeted amount.

1.c We decided to use a commercial lens for the widest field option, rather than a simple plano-convex lens, to retain field flatness and achromatic performance. This also greatly simplified the mechanical design. One of these lenses is used to collimate the beam from **1.b** after the spatial region of interest is selected with the slit.

1.d We added a separate guide telescope rather than a wide field lens for tracking. This telescope is a new one that was made available to this project by the observatory. Its greater focal plane scale than the lens system selected in the preliminary design will give higher quality tracking, and enable stellar spectroscopy. The ability to do that was requested by Dr. Frank Clark. There was no cost to this change.

2.a The 0.25 m spectrograph is the one originally specified. Its acquisition cost was slightly less than budgeted due to discounts from the manufacturer. The instrument is used in two ways in the revised design. It may be coupled with the wide field entrance optics when the computer-controlled rapid wavelength changes it can perform are needed. Alternatively, it may be used with the 0.52 m diameter primary mirror of the Moore Observatory telescope to allow detailed spatially resolved spectroscopy with a field of view about 5 times smaller than the wide field system.

2.b The grating was added to the design in order to improve the angular resolution, when it became apparent that we could design an instrument for this application with higher angular and spectral resolution than originally proposed. This choice of grating eliminated the need for expensive filters. It is used in combination with inexpensive gelatin photographic filters which separate orders.

2.c This adjustable slit is the field stop for the wide field image, and the entrance slit for the spectrograph. It was required for the new design, but we had one on hand from a retired instrument. There was no cost for this addition.

3.a The CCD of first choice was a Kodak 2048 $\times$ 2048 detector with 9 μm square pixels. We decided to change to a different manufacturer for two reasons. First, on testing we found that the Kodak device would not function

with full quantum efficiency at cryogenic temperatures. At elevated operating temperatures its noise level over the anticipated exposure times exceeded a level which we thought was acceptable. Second, the pixel size was too small for the revised optical design, and we would have had to bin pixels 2×2 in order to use it effectively. In the binned mode, the detector would be 1024×1024 with 18 μm pixels. For a lower cost we could obtain a Tektronix thinned, backside illuminated, CCD with exceptionally low noise and an acceptable 25 μm pixel size. The overall cost was also lowered by competitive bidding, with the contract going to Princeton Instruments rather than Photometrics.

3.b After the proposal was approved, Santa Barbara Instrumentation Group announced the availability of a new CCD with 11 μm square pixels rather than the larger, rectangular, pixels which were specified for this tracking camera. We made the substitution because it was lighter and less expensive.

4.a The mounting was designed by us for this instrument. It was machined in the Physics shop by our instrument maker Keith Gowen. There was no charge for the shop time, which totalled over 200 hours. The components are primarily aluminum, brass, and stainless steel. The counterweights are cast gray iron. Miscellaneous materials costs, for example for screws, bearings, and raw materials, are itemized separately in **7.b**. The finished instrument was black satin anodized by a commercial metal finisher at our expense.

4.b The microstepping motors are the ones specified in the proposal.

4.c Three precision rotating stages were added to the instrument. Two stages provide for offset guiding, a feature we added when the decision was made to improve tracking performance. A third stage is used as a grating rotator to permit precise manual adjustment of the instrument's central wavelength. The mounting bayonets for the Nikor lenses are also included in this line.

4.d After consultation with the machinist, we decided that it would be faster, and probably yield a better result, if we purchased commercial drive gears rather than manufacture them ourselves. Two gears, one for each axis, were purchased as a package from Edwin R. Byers Engineering, a company with long experience in manufacturing telescope tracking gear systems.

5.a The control PC base unit price was somewhat less than originally budgeted, primarily due to decreasing prices in the industry. Digital Equipment has a state contract which also lowered our cost further.

5.b The Windows-based Forth operating system was less than budgeted because we obtained it as an upgrade of a system purchased last year.

5.c The tape drive is the one specified in the proposal.

5.d A printer was added to this system when it became apparent that hard-copy listing were essential for developing programs and maintaining data acquisition records.

6.a The workstation is the one specified in the proposal.

6.b System software is provided free by a site license agreement between the University and Digital.

6.c The tape drive is the one specified in the proposal.

6.d A printer was added to the workstation to provide for hardcopies of images. The printer which we selected is the lowest price one that produces good quality gray scale and false color output at a low cost per print. It includes an Ethernet interface for high speed data transfer.

6.e An additional disk drive was added to increase the online storage of image data.

6.f An additional disk drive and CD-ROM drive was added to allow access of this system to the NASA Digitized Sky-Survey.

7.a The NASA Digitized Sky-Survey was added to provide a database of widefield images of the entire sky. These are 1541 digitized photographic images of the Southern Sky taken with the UK Schmidt and of the Northern Sky taken with the Ochsin Schmidt. These images are stored on 102 CD-ROM's and are used by *WISPI* for pointing, object acquisition, and field identification.

7.b One of the options for the use of this instrument is to take it to a remote site in the west, Hawaii, or South America. We included moisture proof, impact resistant, shipping containers for the most critical components.

7.c Small parts and materials for the mounting and cables are subtotaled in this line.

3 Performance

3.1 Introduction

In field tests this fall the completed instrument was used to acquire spectra of the night sky, several bright stars, regions near Jupiter, and nebulae in Lyra, Orion, Monoceros and Pleaides. In this section we review the performance and show examples from these test runs.

3.2 Optical Specifications

The basic characteristics of the instrument are set by the aperture, focal length and resolution of the image forming lens, the dispersion of the spectrometer, and the sensitivity of the detector. These specifications are summarized below.

Primary image forming optical system is a 400 mm f/2.8 Nikor ED (extremely low dispersion glass) lens. The lens is internally focused, and maintains acceptable focus (2 pixels in the detector plane) over a typical spectral coverage of one grating setting. The primary focal plane scale image scale is 516 $''$ /mm.

Alternative image forming system is a 180 mm f/2.8 Nikor ED lens which provides an image scale of 1146 $''$ /mm.

Field of view along the spatial dimension of a 25 mm square detector in the final spectral image plane the primary 400 mm lens is 3.2°. With the alternative shorter focal length lens the field is 7.1°. With the 0.52 m telescope and the Chromex imaging spectrograph the field is 0.61°.

Angular resolution set by two 25 μm pixels in the spectral image plane is 23$''$ with the 400 mm lens, and 51$''$ with the 180 mm lens. The angular resolution measured in the same way with the 0.52 m telescope is 4$''$.

Entrance slit masks the image of the sky along a strip 25 μm wide and 25 mm long. The slit width may be opened to 3 mm for two other modes of operation to acquire objective grating spectra of dense star fields and monochromatic images of extended emission line sources.

Collimator is a 180 mm focal length f/2.8 Nikor ED lens.

Diffraction grating is a 102×102 mm, 300 groove/mm, 7620 Å blaze, Milton Roy precision grating. The peak efficiency is 92% diffracted into the blaze angle.

Spectrograph camera lens is a 200 mm f/2 Nikor ED lens. Combined with the 180 mm collimator, this lens magnifies the image plane by 1.11 times. The use of a large, 100 mm diameter, 200 mm focal length, f/2 lens reduces vignetting at the spectral or spatial edges of the field.

Filters are inserted into the 200 mm f/2 lens close to the spectral image plane. The lens accommodates cut gelatin filters. We use a Wratten 21 which transmits from 5500 Å to 1 μm and blocks second order diffraction from the grating. To cover from 3000 Å to 5500 Å the high pass Wratten 21 filter is removed and replaced with a low pass filter. This allows one grating to be used close to its blaze for all wavelengths from the atmospheric cutoff in the ultraviolet to the detection limit of the CCD in the infrared.

Spectral resolution as set by two pixels and a dispersion of 3.92 Å/pixel in the spectral image plane is 7.8 Å. The actual resolution is one pixel in the regions of best focus.

Spectral coverage at 3.92 Å/pixel is $\approx$4000 Å at one setting of the grating in first order. The instrument typically is set for 5500 Å to 9500 Å. In second order, for the blue, the coverage is half this and the instrument would span 3500 to 5500 Å in one exposure.

Detector The spectral image is detected with a Princeton Instruments CCD camera. It utilizes a Tektronix 1024×1024, 25 μm square pixel, backside illuminated, zero defect, scientific grade CCD. The detector has been overcoated with a proprietary fluorescent dye to extend the response into the ultraviolet. When the CCD is cooled to -120° its output noise is approximately 1 ADU (analog-to-digital unit), or 6.7 e^-. The actual signal noise is determined by photon statistics as described below.

3.3 Vega and Absolute Calibration

The overall system efficiency is wavelength dependent because of the spectral response of the detector, the blaze of the diffraction grating, and the absorption of the optical system. An approximate calibration can be obtained by using the known or specified characteristics of every element in the optical path and multiplying the efficiencies. Because the optical systems are so complex, with dozens of elements and twice as many surfaces, this is inexact. Our expectation was that the efficiency would be of the order of 10% in the red, but very dependent on the quality of the grating and the antireflection characteristics of the lens coatings.

To establish this exactly we will have to make measurements of a photometric standard such as a platinum black body. We have made a preliminary determination by measuring the spectrum of Vega, which has been calibrated

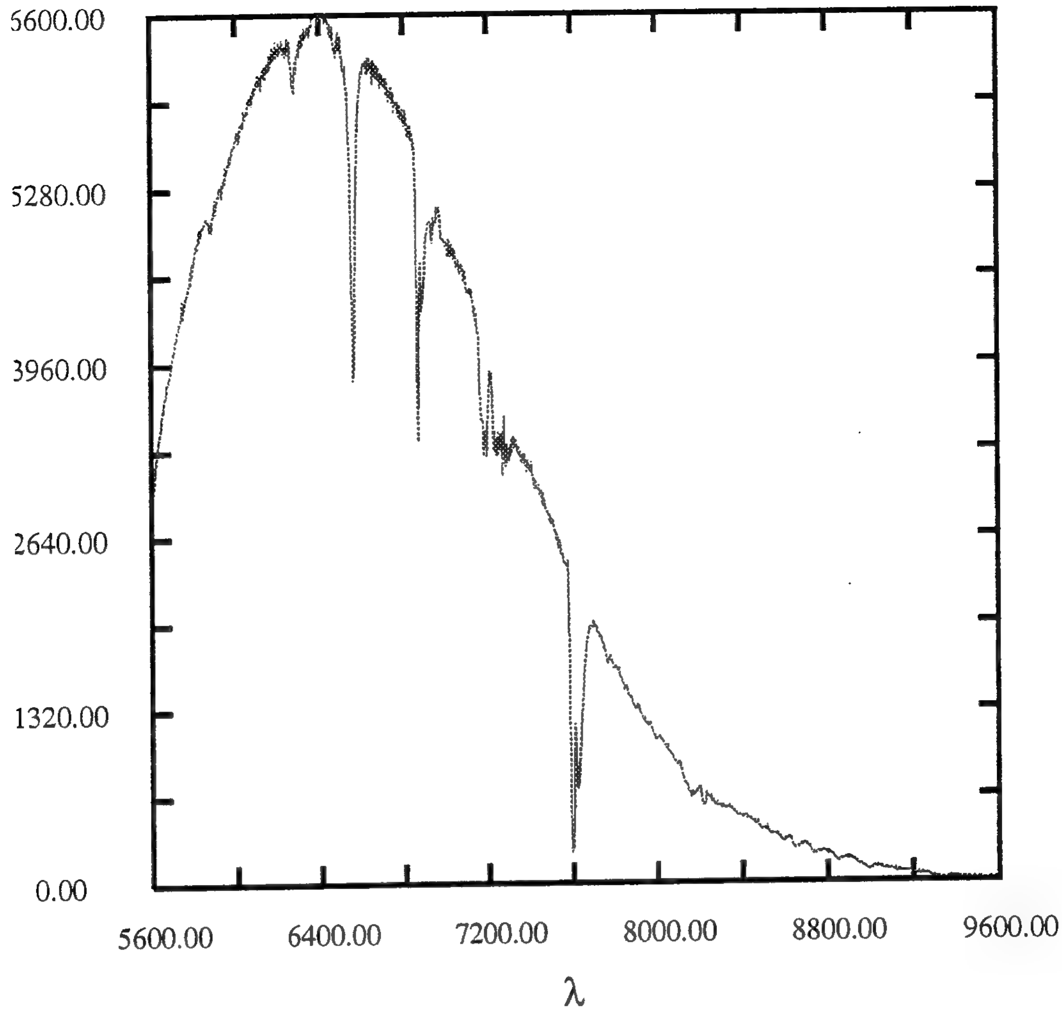

Figure 3: The spectrum of Vega recorded with *WISPI* . The wavelength (λ) scale is in Å; the raw signal is in units of (ADU's) per second. One ADU is equivalent to 6.7 detected photons.

against photometric standards and is itself the astronomical magnitude and color standard. A typical spectrum of Vega taken with a wide slit to avoid light loss at the slit is shown in Fig. 3. We divide this experimental result by the known calibration spectrum to find an instrument response. The Earth's atmospheric transparency is the primary uncertainty in this procedure, and we have not yet compensated for that. The calibration we show in Fig. 4 is referenced to light entering at the top of the Earth's atmosphere. It is apparent from this figure that the peak response is quantum efficiency of 10%, and that the sensitivity is usable sensitivity from the yellow to the near infrared. The short wavelength response should be similar, with a lower peak efficiency because of the lower quantum efficiency of the detector in the blue, and the lower transparency of the atmosphere, the lenses and the order separation filter.

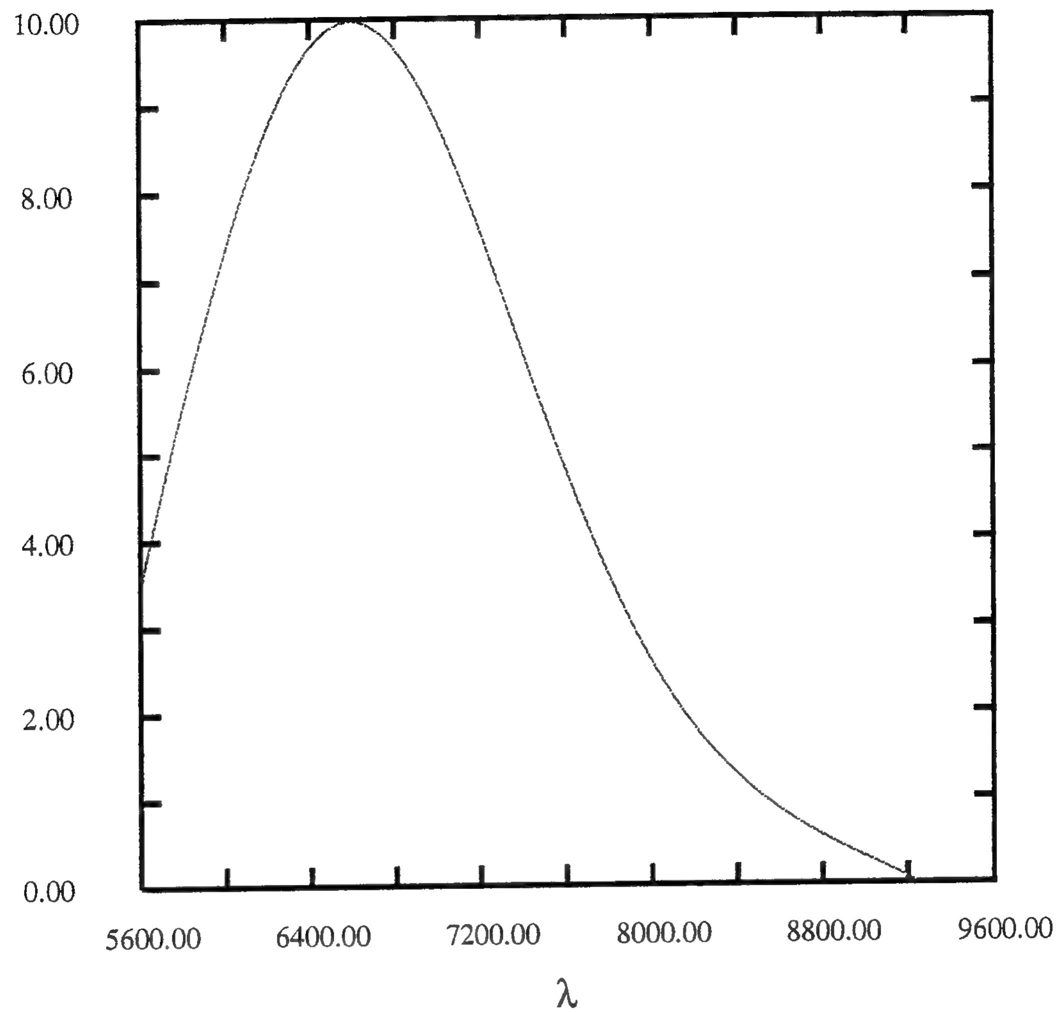

Figure 4: The absolute quantum efficiency (%) of *WISPI* determined from the spectrum of Vega and its known flux, referenced to the top of the Earth's atmosphere. The wavelength (λ) scale is in Å.

3.4 Airglow and Night Sky Spectrum

The ambient night sky spectrum is fairly well understood, although most of the measurements and atlases in the literature are based on photography, or photomultiplier scans, and predate the introduction of sodium lighting. The flux levels for many lines are variable, but stable enough to be used to confirm the instrument's sensitivity. In Fig. 5 we show a fairly typical night sky spectrum. This is a region selected from a wide field spectral image, and summed over an angular width that does not include any identifiable stars. Several of the major features are labeled. The outdoor lighting lines of Na and Hg are particularly apparent because these observations were made only 30 km from Louisville, Kentucky. The strong high pressure Na resonance emission dominates the yellow-red, but in spite of that, all of the air glow emission in the Chamberlain atlas can be seen in this spectrum.

3.5 Nebular Emission in Monoceros

An excellent test of the instrumental characteristics is to use it to record a low surface brightness nebula. For this we chose the *Rosette* in Monoceros which has an angular diameter larger than the full moon. Parts of it are barely visible to the eye with the aid of a richest field telescope under the best of dark sky conditions. To record such a spectrum normally would be a task for very large telescope, which then it would be able only to see a piece of the nebula at a time. The images which we obtained took only 1000 sec for a true spectral image, with the slit along a chord of the roughly circular nebula, and 100 sec for a survey image in Hα light taken with a wide slit. The spectrum of the nebula is shown in Fig. 6. A magnified portion of the wide field spectral image is shown in Fig. 7. This is primarily Hα emission since the underlying [NII] is considerably weaker.

3.6 Resolution and Sensitivity

These and other similar results allow us to determine the angular and spectral resolutions, the lowest signals which we can detect from extended sources, and the limiting magnitude for stellar sources. We consider these briefly in turn.

Angular resolution was expected to be of the order of 2 pixels or 23$''$ when the lens systems were in focus. The uncertainties were the degree of correction for chromatic aberration in the refracting optics, and the off-axis image quality. Stellar spectra can be focused at the center of the field, and remain in focus to within 1 pixel near the outer edges in the sense of angular offset from the center. There is defocusing in the sense of wavelength offset which we attribute to uncorrected chromatic aberration. The effect is largest at the extreme limits, exceeding 2 pixels at the infrared edge of the spectral field. In critical cases it may be desirable to refocus for the wavelengths of interest.

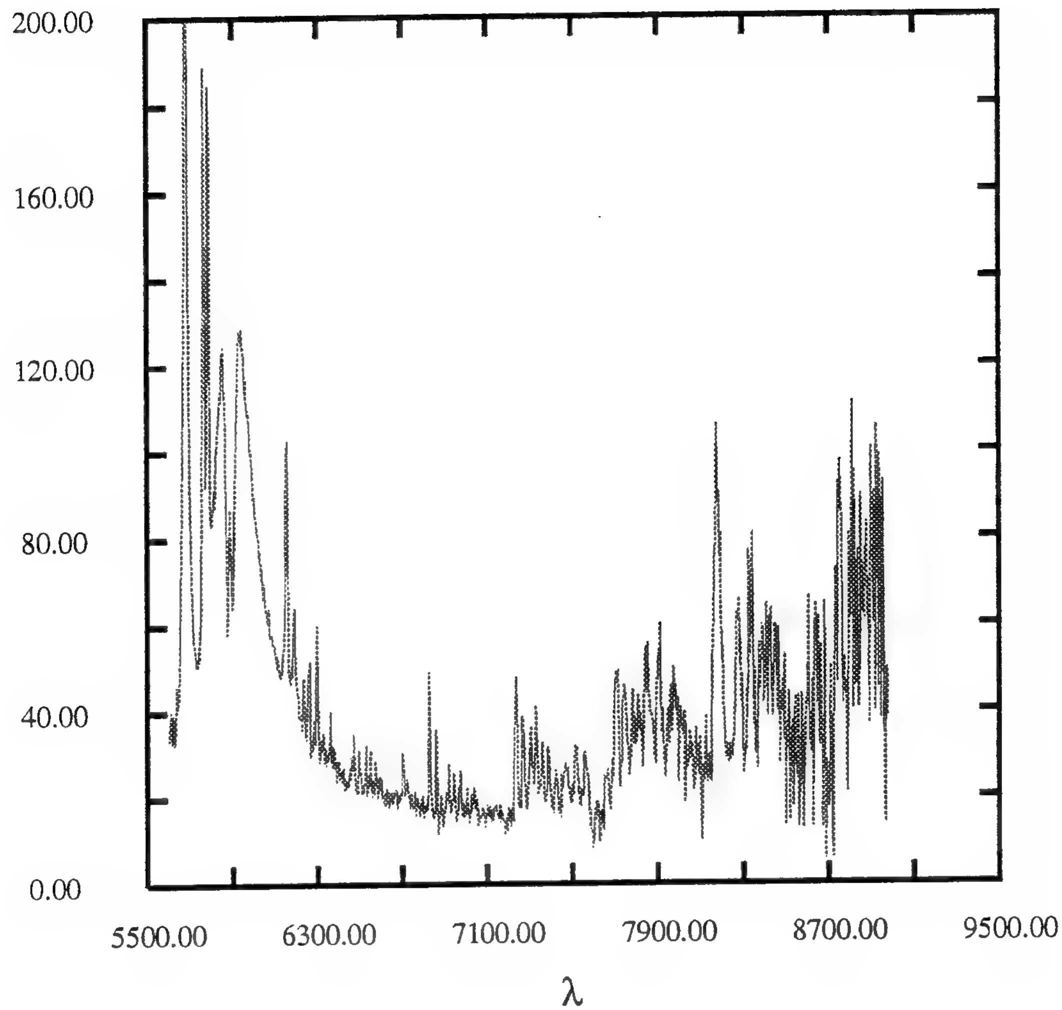

Figure 5: The spectrum of airglow with Na and Hg scattered outdoor lighting from a nearby large city, corrected for instrument response. The wavelength (λ) scale is in Å. The signal scale is in Rayleighs.

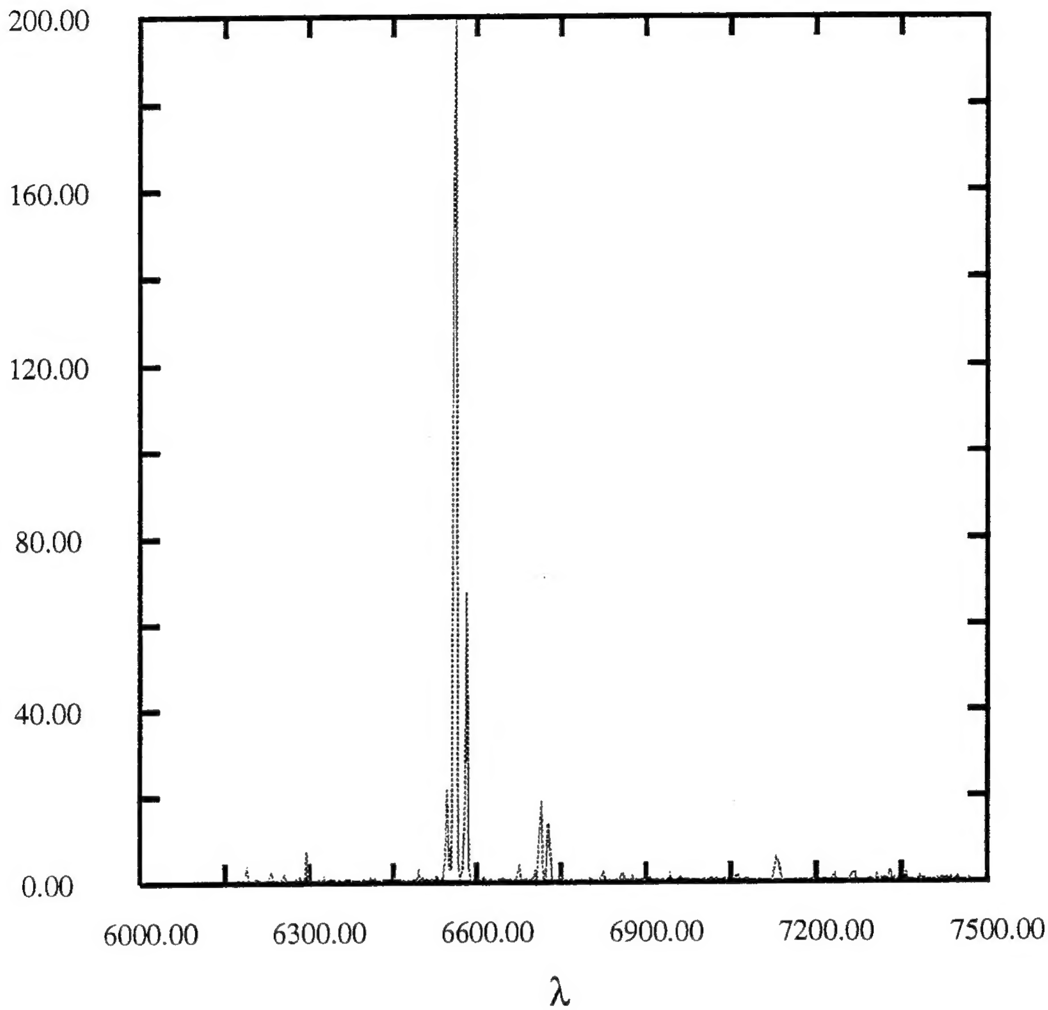

Figure 6: The spectrum of the Rosette Nebula corrected for instrument response. The wavelength (λ) scale is in Å. The signal scale is in units of *photons* per cm^2 at the top of the Earth's atmosphere accumulated over the entire 1000 s exposure. The strongest line is Hα at 6563 Å; it is flanked by weaker lines of [NII].

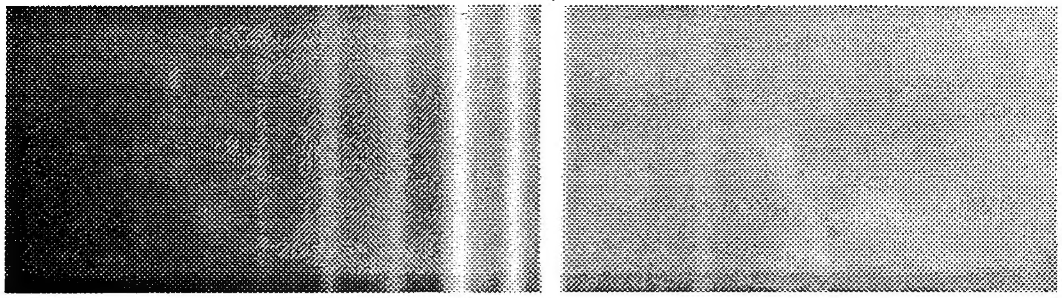

Figure 7: A magnified section of the Hα region of a spectral image of the Rosette with a wide slit. Portions of the Hα structure in the nebula cross the image in this 100 s exposure. The vertical bright lines are stellar continuum emission.

but for survey work this is not necessary. It is necessary to refocus when the instrument is operated in the near ultraviolet instead of the red, as might be expected. On the whole, the anticipated angular resolution of 23″ is obtained at the center of the field with a degradation to $\approx 40''$ at the edges of the field.

Spectral resolution was expected to be of the order of 2 pixels or 7.8 Å at the center of the field. This was achieved. The spectral resolution may degrade to more than 10 Å at 9600 Å, but is generally close to the expected value through the visible and near infrared.

Sensitivity to extended sources is of the order of 1 Rayleigh. We arrive at this estimate in the following way. The forbidden [OI] line at 6300 Å is easily detected in airglow emission (see Fig. 5). A typical signal is 292 ADU's above the bias in a 500 s exposure. With allowance for the calibrated quantum efficiency of the system, this corresponds to 1.75 photons/pixel^2 s, or 43 Rayleighs. (A 1 R source is 10^6 photons/cm^2 s into 4π steradians. Our entrance aperture is 162 cm^2.) J. W. Chamberlain [Physics of the Aurora and Airglow (Academic, New York, 1961)] and A. L. Broadfoot and K. R. Kendall [J. Geophys. Res. **73**, 426 (1968)] quotes values of 50 to 100 R for [OI] which is in line with this measurement given that the emission rate is variable. For comparison, R. J. Reynolds (Ap. J. **282**, 191 (1984)) puts the background emission from galactic Hα at 10 R, roughly the same as atmospheric and geocoronal Hα. A 3600 s exposure, particularly in the absence of Na 5890 Å outdoor lighting contamination, would reach a detectable level of less than 1 R at Hα with an intrinsic noise 2 ADU. With spatial summing this limit could be pushed slightly.

Limiting magnitude is found by referring to a spectrum of Vega, which is a standard 0^{th} magnitude star. At Hα the reference flux for Vega is 6600 ADU's per second, from which we can estimate the magnitude for any measured flux

$$m_\star = -2.5 \log_{10}(F/6600)$$

where F is the flux in ADU/s detected close to Hα. Working backwards, for a 10:1 signal-to-noise ratio we would need at least 10 ADU in a 3600 s exposure. The expression yields $m_\star = 15.9$ for a continuum source. A spatially unresolved line emission source would be much more detectable since the collected photon flux would be concentrated in fewer pixels. A complication, however, is the contribution from airglow and scattered city lighting which was not included in this estimate. A preliminary result is that the sky background contributes about 15 mag/pixel^2 at our local site, mostly from OH in airglow and the continuum emitted by high pressure sodium lamps.

4 Conclusion

The wide field spectral imager which we proposed has been successfully built and tested. The design criteria of sensitivity, spectral and spatial resolution, and spectral and spatial coverage have been met. The completed instrument is capable of rapid wide field measurements of extended celestial background down to a level of $\approx 1 - 2$ R with an angular resolution of ≈ 10 Å on a routine basis. It is also capable of recording the spectra of stars down to 15^{th} magnitude, many at a time in single wide field exposures. Discussions are now underway with Dr. Frank Clark of the Phillips Laboratory regarding the use of this instrument to supply basic measurements as needed.